MULTIPLICITY ANALYSIS OF TWO PARALLEL AND CONSECUTIVE CHEMICAL REACTIONS IN A NON - ISOTHERMAL CATALYST PELLET

Gheorghe Juncu

POLITEHNICA University Bucharest

Department of Chemical and Biochemical Engineering

Polizu 1, 011061 Bucharest

Romania

E-mail: juncu@cael.pub.ro; juncu.gheorghe@yahoo.com

ABSTRACT

The steady-state multiplicity of the porous, non-isothermal, catalyst pellet when two parallel and consecutive chemical reactions take place was analysed in this work. The geometry selected for the catalyst pellet is finite hollow cylinder. A numerical multigrid continuation technique with the preconditioned conjugate gradient squared as coarse grid solver was used. The continuation parameter is the dimensionless adiabatic heat rise (Prater number) for the first chemical reaction. The effect of the other governing parameters was analysed and the results are compared to those provided by the single chemical reaction.

Keywords: Reaction engineering; Catalysis; particle; multiplicity; parallel reactions; consecutive reactions;

Nomenclature

C_A – concentration of the reactant inside the pellet

$C_{A,b}$ – bulk concentration of the reactant

C_B – concentration of the intermediate inside the pellet

D_{eff} – effective diffusivity in the porous catalyst pellet

E_j – activation energy of the jth chemical reaction, j = 1, 2

H – cylinder height

k_j – reaction rate constant for the jth chemical reaction, j = 1, 2

$k_{0,j}$ – pre-exponential factor of the jth chemical reaction, j = 1, 2

r – radial coordinate, cylindrical coordinate system

r^* - dimensionless radial coordinate, $\frac{r - R_i}{R_o - R_i}$

R_G – gas constant

R_i – inner radius of the hollow cylinder

R_o – outer radius of the hollow cylinder

T – temperature of the pellet

T_b – bulk temperature

v_{Rj} – chemical reaction rate for the jth chemical reaction, j = 1, 2

y_A – dimensionless concentration of the reactant inside the pellet, C_A / $C_{A,b}$

y_B – dimensionless concentration of the intermediate inside the pellet, C_B / $C_{A,b}$

z – axial coordinate, cylindrical coordinate system

z^* - dimensionless axial coordinate, 2 z / H, cylindrical coordinate system

Greek Letters

β_j – dimensionless adiabatic heat rise (Prater number), (- $\Delta H_{R,j} D_{eff} C_{A,b}$) / ($\lambda_{eff} T_b$) of the jth chemical reaction, j = 1, 2

χ – geometric ratio, $\frac{R_i}{R_o - R_i}$

γ_j – dimensionless activation energy (Arrhenius number), E_j / R_G T_b, of the jth chemical reaction, j = 1, 2

δ – reaction enthalpy ratio, δ = - $\Delta H_{R,1}$ / - $\Delta H_{R,2}$

$\Delta H_{R,j}$ – enthalpy of the jth chemical reaction, j = 1, 2

ε – aspect ratio, 2 (R_i – R_o) / H

$\eta_{A(B)}$ - effectiveness factor for the species A (B)

θ – dimensionless pellet temperature, T / T_b

λ_{eff} – effective thermal conductivity in the porous catalyst pellet

ρ – bulk density of the pellet

φ_j – reaction parameter (Thiele modulus) for the jth chemical reaction, j = 1, 2

1. Introduction

Under certain conditions, chemically reacting systems exhibit multiple steady states. Steady - state multiplicity is defined by: for the same values of the input variables, different steady states result from different initial conditions. The steady - state multiplicity provides useful information for the expression of the chemical reaction rate and has an important impact on the design, start-up and control of chemical reactors.

One of the chemically reacting systems for which the steady - state multiplicity was widely investigated is the catalyst pellet. Reviews on this subject can be viewed in Luss (1987) and Luss and Sheintuch (2005). However, in the almost all the articles published in this topic a single chemical reaction was considered. In spite of the fact that most practical problems associated with steady – state multiplicity are encountered in multi – reactions systems, less attention has been given to the multiplicity analysis of the complex chemical reactions in catalyst pellets. The multiplicity of the steady states for parallel and consecutive chemical reactions was studied for chemically reacting systems modelled by lumped parametric mathematical models.

Hlavacek et al. (1972) derived the regions of multiplicity, stability of steady states, behavior of limit cycles, shapes of separatrices for a non-isothermal CSTR with exothermic consecutive first order reactions. The same problem was analysed later by Farr and Aris (1986). The steady - state multiplicity of a non-isothermal CSTR with parallel chemical reactions was investigated by Luss and Chen (1975) and Balakotaiah and Luss (1983). Elnashaie (1977) analysed, for a simple lumped parametric model of a fluidized bed chemical reactor, the implications of the multiplicity phenomenon on the selectivity and

yield of the desired intermediate product of the exothermic consecutive first order reaction. Pikios and Luss (1979) and Balakotaiah and Luss (1982) derived exact criteria for predicting the conditions under which steady – state multiplicity occurs in lumped parameter systems in which either two consecutive or two parallel reactions occur. Based on the theoretical predictions of a lumped parametric model for the catalyst pellet, Harold and Luss (1985) studied experimentally the steady - state multiplicity for the case of a parallel chemical reaction. Elnashaie et al. (1993) analysed the bifurcation, instability and chaotic characteristics for the non – isothermal fluidized bed catalytic reactor with consecutive, first – order exothermic chemical reactions. The steady-state multiplicity for consecutive biochemical reactions in a CSTR was studied by Volcke et al. (2010). The analysis of the steady – state multiplicity for a non – isothermal consecutive reaction taking place in fluidized – bed autothermal structures was recently made by Bizon (2017).

The multiplicity of the steady states for the reactor – separator – recycle system in which a complex chemical reaction occur was investigated by:

(1) Bildea et al. (2000); isothermal first order consecutive chemical reaction taking place in a CSTR or a plug flow reactor (PFR);

(2) Kiss et al. (2005); isothermal, second – order parallel / consecutive and parallel reactions taking place in a CSTR;

(3) Altimari and Bildea (2008, 2009); non-isothermal consecutive reactions taking place in a PFR.

For a distributed parametric mathematical model, the steady - state multiplicity of the catalyst pellet for parallel and consecutive chemical reactions was not investigated until now. This work wishes to fill this gap by computing the bifurcation diagrams for parallel

and consecutive chemical reactions taking place in a catalyst pellet. The geometry selected for the catalyst pellet is the finite hollow cylinder (the widely used shape according to Wijngaarden et al., 1998). The chemical reactions are considered first-order irreversible and the inter-phase gradients were neglected.

2. Mathematical Model

Consider a finite hollow cylindrical catalyst pellet with internal / external radius R_i / R_o and height H. Inside the particle, the non-isothermal, first-order irreversible parallel or consecutive chemical reactions,

- Parallel reactions

$$A \rightarrow B,\ v_{R1} = k_1 C_A$$

$$A \rightarrow F,\ v_{R2} = k_2 C_A$$

- Consecutive reactions

$$A \rightarrow B,\ v_{R1} = k_1 C_A$$

$$B \rightarrow F,\ v_{R2} = k_2 C_B$$

take place. The chemical species A transfers into the particle from the surrounding fluid. The inter-phase transport resistances are assumed negligibly (the concentration and temperature on the external surface of the catalyst pellet are the same as the bulk values). Considering a homogeneous porous pellet and using effective transport coefficients (Aris, 1975), the steady state concentration and temperature profiles inside the hollow cylinder are given by:

- Parallel reactions

$$D_{eff}\Delta C_A - \rho \left[k_{0,1}\, exp\left(-\frac{E_1}{R_G T}\right) + k_{0,2}\, exp\left(-\frac{E_2}{R_G T}\right)\right] C_A = 0 \quad (1a)$$

$$\lambda_{eff}\,\Delta T + \rho \left[-\Delta H_{R,1}\, k_{0,1} exp\left(-\frac{E_1}{R_G T}\right) - \Delta H_{R,2}\, k_{0,2}\, exp\left(-\frac{E_2}{R_G T}\right)\right] C_A = 0 \quad (1b)$$

- Consecutive reactions

$$D_{eff}\,\Delta C_A - \rho\, k_{0,1}\, exp\left(-\frac{E_1}{R_G T}\right) C_A = 0 \quad (1c)$$

$$D_{eff}\,\Delta C_B + \rho\, k_{0,1}\, exp\left(-\frac{E_1}{R_G T}\right) C_A - \rho\, k_{0,2}\, exp\left(-\frac{E_2}{R_G T}\right) C_B = 0 \quad (1d)$$

$$\lambda_{eff}\,\Delta T + \rho \left[-\Delta H_{R,1}\, k_{0,1} exp\left(-\frac{E_1}{R_G T}\right) C_A - \Delta H_{R,2}\, k_{0,2}\, exp\left(-\frac{E_2}{R_G T}\right) C_B\right] = 0 \quad (1e)$$

where

$$\Delta = \frac{1}{r}\frac{\partial}{\partial r}\left(r \frac{\partial}{\partial r}\right) + \frac{\partial^2}{\partial z^2}$$

When the inter-phase gradients are neglected, the boundary conditions are:

- $r = R_i$;

$$C_A = C_{A,b},\ C_B = C_{B,b},\ T = T_b \quad (2a)$$

- $r = R_o$;

$$C_A = C_{A,b},\ C_B = C_{B,b},\ T = T_b \quad (2b)$$

- $z = 0$;

$$\frac{\partial C_A}{\partial z} = \frac{\partial C_B}{\partial z} = \frac{\partial T}{\partial z} = 0 \quad (2c)$$

- $z = H / 2$;

$$C_A = C_{A,b},\ C_B = C_{B,b},\ T = T_b. \quad (2d)$$

The origin of the cylindrical coordinate system (r, z) is placed in the centre of the particle. The characteristic length used is the difference between the outer radius and the inner radius of the hollow cylinder, $R_o - R_i$.

Defining the dimensionless variables and groups

$$r^* = \frac{r - R_i}{R_o - R_i} \qquad \chi = \frac{R_i}{R_o - R_i} \qquad z^* = 2\,z\,/\,H$$

$$y_A = \frac{C_A}{C_{A,b}} \quad y_B = \frac{C_B}{C_{A,b}} \quad \theta = \frac{T}{T_B} \quad \varepsilon = 2\,\frac{R_o - R_i}{H}$$

$$\beta_j = \frac{-\Delta H_{R,j}\, D_{eff}\, C_{A,b}}{\lambda_{eff}\, T_b} \quad \gamma_j = \frac{E_j}{R_G\, T_b} \quad \varphi_j = (R_o - R_i)\sqrt{\frac{\rho\, k_{0,j}\, exp(-\gamma_j)}{D_{eff}}} \quad j = 1, 2$$

$$\delta = \frac{\beta_2}{\beta_1} = \frac{-\Delta H_{R,2}}{-\Delta H_{R,1}}$$

the non-dimensional form of (1) is

- parallel reactions

$$\Delta^* y_A - y_A \left\{ \varphi_1^2\, exp\left[\gamma_1 \left(1 - \frac{1}{\theta}\right)\right] + \varphi_2^2\, exp\left[\gamma_2 \left(1 - \frac{1}{\theta}\right)\right]\right\} = 0 \qquad (3a)$$

$$\Delta^* \theta + \beta_1\, y_A \left\{ \varphi_1^2\, exp\left[\gamma_1 \left(1 - \frac{1}{\theta}\right)\right] + \delta\, \varphi_2^2\, exp\left[\gamma_2 \left(1 - \frac{1}{\theta}\right)\right]\right\} = 0 \qquad (3b)$$

- consecutive reactions

$$\Delta^* y_A - \varphi_1^2\, y_A\, exp\left[\gamma_1 \left(1 - \frac{1}{\theta}\right)\right] = 0 \qquad (3c)$$

$$\Delta^* y_B + \varphi_1^2\, y_A\, exp\left[\gamma_1 \left(1 - \frac{1}{\theta}\right)\right] - \varphi_2^2\, y_B\, exp\left[\gamma_2 \left(1 - \frac{1}{\theta}\right)\right] = 0 \qquad (3d)$$

$$\Delta^* \theta + \beta_1 \left\{ \varphi_1^2\, y_A\, exp\left[\gamma_1 \left(1 - \frac{1}{\theta}\right)\right] + \delta\, \varphi_2^2\, y_B\, exp\left[\gamma_2 \left(1 - \frac{1}{\theta}\right)\right]\right\} = 0 \qquad (3e)$$

where

$$\Delta^* = \frac{\partial^2}{\partial r^{*2}} + \frac{1}{\chi + r^*}\frac{\partial}{\partial r^*} + \varepsilon^2\,\frac{\partial^2}{\partial z^{*2}}$$

with the boundary conditions

- $r^* = 0$;

$$y_A = \theta = 1, y_B = 0 \tag{4a}$$

- $r^* = 1$;

$$y_A = \theta = 1, y_B = 0 \tag{4b}$$

- $z^* = 0$;

$$\frac{\partial y_A}{\partial z^*} = \frac{\partial y_B}{\partial z^*} = \frac{\partial \theta}{\partial z^*} = 0 \tag{4c}$$

- $z^* = 1$;

$$y_A = \theta = 1, y_B = 0 \tag{4d}$$

The quantities of interest used in this work are:

- pellet average dimensionless temperature, $\bar{\theta}$:

$$\bar{\theta} = \frac{2}{1+2\chi} \int_0^1 \int_0^1 \left(r^* + \chi\right) \theta \, d r^* \, d z^* \tag{5a}$$

- pellet average dimensionless concentration, $\bar{y}_A, \bar{y}_B$:

$$\bar{y}_{A\,(B)} = \frac{2}{1+2\chi} \int_0^1 \int_0^1 \left(r^* + \chi\right) y_{A\,(B)} \, d r^* \, d z^* \tag{5b}$$

- effectiveness factor, $\eta_{A(B)}$, for the species A (B)

- parallel chemical reactions

$$\eta_A = \frac{2}{1+2\chi} \frac{1}{\varphi_1^2 + \varphi_2^2} \int_0^1 \int_0^1 \left(r^* + \chi\right) y_A \left\{ \varphi_1^2 \, exp\left[\gamma_1 \left(1 - \frac{1}{\theta}\right)\right] + \varphi_2^2 \, exp\left[\gamma_2 \left(1 - \frac{1}{\theta}\right)\right]\right\} d r^* \, d z^* \tag{5c}$$

- consecutive chemical reactions

$$\eta_A = \frac{2}{1+2\chi} \int_0^1 \int_0^1 \left(r^* + \chi\right) y_A \, exp\left[\gamma_1 \left(1 - \frac{1}{\theta}\right)\right] d r^* \, d z^* \tag{5d}$$

$$\eta_B = \frac{2}{1+2\chi}\frac{1}{\varphi_1^2}\int_0^1\int_0^1 (r^* + \chi)\left\{\varphi_1^2\, y_A exp\left[\gamma_1\left(1-\frac{1}{\theta}\right)\right] - \varphi_2^2\, y_B exp\left[\gamma_2\left(1-\frac{1}{\theta}\right)\right]\right\} d\,r^*\, d\,z^* \quad (5e)$$

The mathematical model equations (3) were discretized with the standard, central second-order accurate, finite difference scheme on grids with N x N points and steps sizes $h_r = h_z = h = 1 / (N\text{-}1)$. The discrete approximation reads as,

$$G\,(u, p) = B\,u - p\,g\,(u) = 0 \quad (6)$$

where $u \in R^n$ corresponds to the field variables, $p \in R$ is the parameter of interest, B an $n \times n$ matrix and g: $R^n \rightarrow R^n$ a smooth mapping.

3. Numerical Methods

The branch of solutions for equation (6) was computed using a continuation technique (Seydel and Hlavacek, 1987), (Allgower and Georg, 1997). The algorithm is presented in detail in Juncu et al. (2006) and Juncu (2007, 2014). For this reason, only a very brief description can be seen in the next paragraphs.

The extended system used by the continuation technique is:

$$G\,(u, p) = 0 \quad (7a)$$

$$N\,(u, p, s) = 0 \quad (7b)$$

where (7b) is given by (Dinar and Keller, 1989):

$$N(u,p,s) \equiv \left[\left\|u-u^{(0)}\right\|^2 + \left(p-p^{(0)}\right)^2\right]^{1/2} - \delta\, s \quad (8)$$

If $u^{(0)}$ ($s^{(0)}$), $p^{(0)}$ ($s^{(0)}$) are the solution of (7) and δs the continuation step in s, the new solution is calculated as following:

- Predictor Step, (Dinar and Keller, 1989)

$$\bar{u} = u^{(0)} + (\delta s)\frac{u^{(0)} - u^{(-1)}}{(\delta s)^{(0)}} \tag{9a}$$

$$\bar{p} = p^{(0)} + (\delta s)\frac{p^{(0)} - p^{(-1)}}{(\delta s)^{(0)}} \tag{9b}$$

- Corrector Step

Newton method applied to (7).

Iterative methods (Preconditioned Conjugate Gradient Squared, PCGS, algorithm, Sonneveld, 1989) were used as linear solver in a Newton step. The continuation algorithm acts on a single, coarse grid. The coarse grid solution is refined by the following MG method (FAST type algorithms, Hackbusch, 1982):

(i) the parameter p is changed only on the coarse grid where the enlarged system (7a, b) is solved; the coarse grid equation should include the fine grid residuals of all equations;

(ii) on fine grids only equation (7a) is smoothed.

The computation starts at low values of p with a usual continuation algorithm. After few steps, the program switches to the continuation procedures described previously with δs calculated from the last solutions. The technique for automatically changing the step length δs is presented in Juncu et al. (2006). The algorithms described previously gave a way for

passing through bifurcation points. To accurately locate the critical points, the alternative approach, based on Cayley transform and power iteration, was used in this work.

The numerical performances of the algorithm are practically the same with those reported in Juncu (2007, 2014). The present numerical results were obtained on a mesh with 65 × 65 points.

4. Results

The dimensionless mathematical model (5) depends on eight non-dimensional parameters: β_1, $\gamma_{1(2)}$, δ, χ, ε^2 and $\varphi^2_{1(2)}$. In all simulations, the Prater number β_1 was the continuation parameter and takes values in the range, $0 < \beta_1 \leq 0.8$ (Aris, 1975 and Froment et al., 2011). The dimensionless activation energies, $\gamma_{1(2)}$ and the dimensionless reaction parameters, $\varphi^2_{1(2)}$ take values in the range (Aris, 1975 and Froment et al., 2011), $0 < \gamma_{1(2)} \leq 28$, $0.1 \leq \varphi^2_{1(2)} \leq 10$. For ε and χ the same values as in Juncu (2014) were used, i.e. $0.1 \leq \varepsilon \leq 10$ and $10^{-4} \leq \chi \leq 10^2$. The values considered for the ratio δ are, $\delta = \pm 0.7, \pm 0.5, \pm 0.3, \pm 0.1$.

The number of parameters for the mathematical model of the complex chemical reactions is greater than the number of parameters of the mathematical model of the single chemical reaction. The increase in the number of parameters increases the number of steady state solutions. The search for the maximum number of the steady state solutions was one the main targets of the articles that investigated the bifurcation behavior of complex chemical reactions for lumped parameter models.

For the present mathematical model, an infinite number of steady state solutions exists even for the case of the single chemical reaction. Thus, the analysis of the increase in the number of steady state solutions cannot be an aim for the present study. The present study starts from the following observation draw by Hlavacek et al. (1972): *an analogy always exists between the single and consecutive exothermic reactions*. The Hlavacek analogy is used in this work for both parallel and consecutive chemical reactions. Concretely, the present investigation consists of: for a given set of reaction parameters and different values of the geometric groups, the bifurcation diagrams of the complex chemical reactions calculated for $-0.7 \leq \delta \leq 0.7$ are compared with the bifurcation diagram of the single chemical reaction. The case when one of the chemical reactions is exothermic and the other endothermic is also investigated. In the vicinity of the critical boundaries, it is obvious that differences exist between the results provided by the single chemical reaction and the complex chemical reactions. For this reason, the comparison between the bifurcation diagrams of the complex chemical reactions and the single chemical reaction will be performed for parameters values far from the critical boundaries.

4.1 *Parallel Reaction*

From the numerical experiments made, the bifurcation diagrams computed for $\varphi_1^2 = 0.4$; $\varphi_2^2 = 0.3$; $\gamma_1 = 20$; $\gamma_2 = 18$ were selected to be presented in this section. The values of the reaction parameters for the single chemical reaction are: $\gamma = 20$, $\varphi^2 = 0.4$. Figures 1 ($\varepsilon = 1$, $\chi = 1$) and 2 ($\varepsilon = 0.1$, $\chi = 1$) show the case when the exothermic parallel and single chemical reactions have the same bifurcation diagrams. The bifurcation diagrams of the exothermic parallel and single chemical reactions presented in figure 1 are of the type 1 –

3 – 1 (only two turning points were detected). Bifurcation diagrams with an infinite number of steady state solutions for both exothermic parallel and single chemical reactions are plotted in figure 2. Figures 1 and 2 show that for the parallel chemical reactions the increase in δ decreases the β_1 values at the ignition and extinction points. The bifurcation diagram of the exothermic single chemical reaction can be viewed as an approximate envelope of the bifurcation diagrams of the exothermic parallel chemical reactions. However, the differences between the values of β_1 at the ignition and extinction points for the parallel and singular reactions are not negligible.

For the parameter values used in figures 1 and 2 multiple steady states exist for the parallel chemical reactions even when the second chemical reaction is endothermic. Figure 2 shows multiple steady states (an infinite number of steady states) for δ = -0.3. For the case depicted in figure 1 multiple steady states occur when δ < -0.3 (the bifurcation diagrams are of the type 1 – 3 – 1). To avoid too many curves on the same graph, the bifurcation diagrams obtained for $\delta = \pm 0.5$ and $\delta = \pm 0.1$ are not plotted on figures 1 and 2. The bifurcation diagrams obtained for negative values of δ do not intersect with the bifurcation diagrams of the exothermic single chemical reactions. In this case, the bifurcation diagram of the exothermic single chemical reaction cannot be considered an approximate envelope of the bifurcation diagrams of the parallel chemical reactions. However, for the cases presented in figures 1 and 2, one may consider the Hlavacek analogy valid.

Figure 3 (ε = 0.1, $\chi = 10^{-4}$) shows the case when, for the exothermic parallel chemical reactions, the increase in δ changes the type of bifurcation diagram from a diagram with an infinite number of steady states (δ = -0.3) to a diagram of the type 1 – 3 –

1 (δ = 0.3, 0.7). The single chemical reaction exhibits a bifurcation diagram with an infinite number of steady states. For $\chi \rightarrow 0$ the hollow cylinder solutions tend to the solid cylinder solutions. The numerical simulations made shown that, for the same values of the reaction parameters and the geometric parameter ε, the solid cylinder does not exhibit multiple steady states at δ = 0.3 and δ = 0.7.

When $\delta < 0$ and δ decreases, the change of the path of solutions from a complex case that exhibits multiple steady states to a simple case when multiplicity does not occur is an expected phenomenon. The change of the path of solutions from a complex diagram to a simple one when $\delta > 0$ and δ increases cannot be considered an expected phenomenon. Usually, the increase in the exothermicity of the system should increase the complexity of the bifurcation diagram.

Numerical simulations were made for other values of the reaction parameters. If the reaction parameters are selected such that there are significant differences between the reaction rates of the two chemical reactions (the rate of the second reaction is significantly smaller than the rate of the first reaction), the bifurcation diagrams for the parallel reaction overlap on the bifurcation diagram of the single chemical reaction. When the rates the two reactions are comparable, bifurcation diagrams similar to those presented in figures 1 – 3 were obtained. Cases when the Hlavacek analogy is valid for all values of the geometric parameters used in this section were encountered. For example, the case: for φ_1^2 = 0.3; φ_2^2 = 0.2; γ_1 = 20; γ_2 = 18. However, even in this case, the bifurcation diagrams of the solid cylinder (1 – 3 – 1) are different from those of the hollow cylinder for ε = 0.1, $\chi = 10^{-4}$ (infinite number of steady states).

4.2 *Consecutive Reaction*

Bifurcation diagrams computed for the consecutive chemical reaction are presented in figures 4, 5 and 6. For the data plotted in figures 4 - 6 the numerical values of the parameters are identical to those used in figures 1, 2 and 3. Figures 4 - 6 show that:

- The consecutive chemical reaction and the single chemical reaction exhibit the same bifurcation behavior;
- The exothermic – endothermic consecutive chemical reaction has multiple steady states for all δ values used in this work; as for the parallel chemical reaction, the increase in δ decreases the β_1 values at the ignition and extinction points;
- The bifurcation diagram of the single chemical reaction can be viewed as a separatrix between the bifurcation diagrams of the exothermic consecutive chemical reactions and the bifurcation diagrams of the consecutive exothermic – endothermic chemical reactions;

It must be mentioned that the solid cylinder exhibits the same bifurcation behaviour as the hollow cylinder for $\chi = 10^{-4}$.

Numerical simulations were made for other values of the reaction parameters (including the cases $\varphi_1^2 = \varphi_2^2$; $\gamma_1 = \gamma_2$ and $\varphi_1^2 < \varphi_2^2$; $\gamma_1 < \gamma_2$). When the differences between the reaction parameters of the two chemical reactions are relatively small, the consecutive reaction bifurcation diagrams overlap on the bifurcation diagram of the single chemical reaction (situation similar to that encountered at the parallel reaction). If the rates the two reactions are comparable, bifurcation diagrams similar to those presented in figures 4 – 6

were obtained. The numerical simulations made have been show that, from the point of view of Hlavacek analogy, the bifurcation behaviour of the consecutive reaction is most stable versus the variation of the reaction parameters than that of the parallel reaction.

For the consecutive chemical reaction an important quantity that deserves to be analysed is the yield / selectivity in the intermediate species *B*. Bifurcation diagrams for the yield in the intermediate species *B* are presented in figures 7 – 9. The values for the reaction and geometric parameters are the same as in figures 4 – 6. Figures 7 – 9 show that:

- In all cases, the maximum value of the average yield in the intermediate species *B* is placed at the extinction point;
- The increase in δ decreases the numerical values of y_B and implicitly the maximum value of y_B.

The bifurcation diagrams for the effectiveness factor η_B are presented in figures 10 – 12 for the same values of the reaction and geometric parameters. Figures 10 – 12 show that η_B exhibits the same bifurcation behaviour as the dimensionless average temperature. It increases very fast after the extinction point when both chemical reactions are exothermic. The fast increase in η_B corresponds to the fast increase in the pellet dimensionless temperature and the decrease in the yield of the intermediate species *B*.

5. Conclusions

The bifurcation diagrams of a non-isothermal finite hollow cylinder catalyst pellet were calculated for the first-order parallel and consecutive chemical reactions. The external

gradients are neglected. A numerical MG continuation technique with pseudo-arc-length parametrization was applied to the finite difference approximation of the mathematical model.

Starting from the Hlavacek's observation, e.g. *an analogy always exists between the single and consecutive exothermic reactions*, the bifurcation diagrams of the parallel and consecutive chemical reactions were compared to the bifurcation diagrams of the single chemical reaction. The bifurcation diagram of the single chemical reaction intersects the bifurcation diagrams of the exothermic parallel chemical reactions. For the consecutive chemical reaction, the bifurcation diagram of the single chemical reaction is a separatrix between the bifurcation diagrams of the exothermic and exothermic – endothermic reactions. For both parallel and consecutive reactions, multiple steady states were observed for the case of exothermic – endothermic chemical reactions. For consecutive chemical reactions, when multiplicity is present, the maximum value of the yield in the intermediate species *B* is located at the extinction point.

REFERENCES

Allgower, E.L., Georg, K., 1997. Numerical Path Following. In P.G. Ciarlet and J.L. Lions (eds.), Handbook of Numerical Analysis, *Vol. 5*, Amsterdam: North-Holland. available on line from *http://www.math.colostate.edu/emeriti/georg/georg.publications*.

Altimari, P., Bildea, C.S., 2008. Coupling exothermic and endothermic reactions in plug-flow reactor – separation – recycle systems. Ind. Eng. Chem. Res. 47, 6685 – 6697.

Altimari, P., Bildea, C.S., 2009. Integrated design and control of plantwide systems coupling exothermic and endothermic reactions. Comput. Chem. Eng. 33, 911 – 923.

Aris, R., 1975. The Mathematical Theory of Diffusion and Reaction in Permeable Catalysts, Calendron Press, Oxford.

Balakotaiah, V., Luss, D., 1982. Exact steady-state multiplicity criteria for two consecutive or parallel reactions in lumped – parameter systems. Chem. Eng. Sci. 37, 433 – 445.

Balakotaiah, V., Luss, D., 1983. Multiplicity features of reacting systems. Dependence of the steady-states of a CSTR on the residence time. Chem. Eng. Sci. 38, 1709 – 1721.

Bildea, C.S., Dimian, A.C., Iedema, P.D., 2000. Nonlinear behavior of reactor – separator – recycle systems. Comput. Chem. Eng. 24, 209 – 215.

Bizon, K., 2017. Steady – state characteristics of autothermal structures with fluidized – bed catalytic reactors. Chem. Eng. J. 321, 286 – 300.

Dinar, N., Keller, H.B., 1989. Computations of Taylor vortex flows using multigrid continuation methods. Lecture Notes in Engineering 43, Springer, Berlin, 191-262.

Elnashaie, S.S.E.H., 1977. Multiplicity of the steady state in fluidized bed reactors – III, Yield of the consecutive reaction A→ B → C. Chem. Eng. Sci. 32, 295 – 301.

Elnashaie, S.S., Abashar, M.E., Teymour, F.A., 1993. Bifurcation, instability and chaos in fluidized bed catalytic reactors with consecutive exothermic chemical reactions. Chaos, Solitons & Fractals 3, 1 – 33.

Farr, W.W., Aris, R., 1986. Yet who would have thought the old man to have had so much blood in him ? – Reflections on the multiplicity of steady states of the stirred tank reactor. Chem. Eng. Sci. 41, 1385 – 1402.

Froment, G., Bischoff, K.B., De Wilde, J., 2011. Chemical Reactor Analysis and Design (3rd Ed.), Wiley, New York.

Hackbusch, W., 1982. Multi-grid solution of continuation problems. Lecture Notes in Mathematics 953. Springer, Berlin, pp. 20 - 43.

Harold, M.P., Luss, D., 1985. An experimental study of steady – state multiplicity features of two parallel catalytic reactions. Chem. Eng. Sci. 40, 39 – 52.

Hlavacek, V., Kubicek, M., Visnak, K., 1972. Modelling of chemical reactors – XXVI Multiplicity and stability analysis of a continuous stittrd tank reactor with exothermic consecutive reactions A→ B → C. Chem. Eng. Sci.27, 719 – 742.

Juncu, Gh., Mosekilde, E., Popa, C., 2006. Numerical experiments with MG continuation algorithms. Appl. Num. Math. 56, 844 – 861.

Juncu, Gh., 2007. Multiplicity analysis of a nonisothermal finite cylindrical catalyst pellet, Int. J. Heat Mass Transfer 50, 2038 – 2050.

Juncu, Gh., 2014. Multiplicity analysis of a non - isothermal finite hollow cylindrical catalyst pellet, Chem. Eng. Res. Design 92, 954 – 960.

Kiss, A.A., Bildea, C.S., Dimian, A.C., Iedema, P.D., 2005. Design of recycle systems with parallel and consecutive reactions by nonlinear analysis. Ind. Eng. Chem. Res. 44, 576 – 587.

Luss, D., Chen, G.T., 1975. Steady state multiplicity of lumped parameter systems in which two parallel chemical reactions occur. Chem. Eng. Sci. 30, 1483 – 1495.

Luss, D., 1987. Diffusion – reaction interactions in catalyst pellets. In J. Carberry, A. Varma (eds.), Chemical Reaction and Reactor Engineering, Marcel Dekker, New York.

Luss, D., Sheintuch, M., 2005. Spatiotemporal patterns in catalytic systems. Catalysis Today 105, 254 – 274.

Pikios, C.A., Luss, D., 1979. Steady – state multiplicity of lumped – parameter systems in which two consecutive or two parallel irreversible first – order reactions occur. Chem. Eng. Sci. 34, 919 – 927.

Seydel, R., Hlavacek, V., 1987. Role of continuation in engineering analysis. Chem. Eng. Sci. 42, 1281-1295.

Sonneveld, P., 1989. CGS, A fast Lanczos – type solver for nonsymmetric linear systems. SIAM J. Sci. Statist. Comput. 10, 36-52.

Volcke, E.I.P., Sbarciog, M., Noldus, E.J.L., De Baets, B., Loccufier, M., 2010. Steady state multiplicity of two – step biological conversion systems with general kinetics. Math. Biosci. 228, 160 – 170.

Wijngaarden, R.J., Kronberg, A., Westerterp, K.R., 1998. Industrial Catalysis: Optimizing Catalysts and Processes, Wiley VCH, Weiheim.

Figures Captions

Figure 1. Bifurcation diagrams for parallel chemical reactions; φ_1^2 = 0.4; φ_2^2 = 0.3; γ_1 = 20; γ_2 = 18; ε = 1; χ = 1.

Figure 2. Bifurcation diagrams for parallel chemical reactions; φ_1^2 = 0.4; φ_2^2 = 0.3; γ_1 = 20; γ_2 = 18; ε = 0.1; χ = 1.

Figure 3. Bifurcation diagrams for parallel chemical reactions; φ_1^2 = 0.4; φ_2^2 = 0.3; γ_1 = 20; γ_2 = 18; ε = 0.1; $\chi = 10^{-4}$.

Figure 4. Bifurcation diagrams for consecutive chemical reactions; φ_1^2 = 0.4; φ_2^2 = 0.3; γ_1 = 20; γ_2 = 18; ε = 1; χ = 1.

Figure 5. Bifurcation diagrams for consecutive chemical reactions; φ_1^2 = 0.4; φ_2^2 = 0.3; γ_1 = 20; γ_2 = 18; ε = 0.1; χ = 1.

Figure 6. Bifurcation diagrams for consecutive chemical reactions; φ_1^2 = 0.4; φ_2^2 = 0.3; γ_1 = 20; γ_2 = 18; ε = 0.1; $\chi = 10^{-4}$.

Figure 7. Bifurcation diagrams for the yield of the intermediate product, y_B, of the consecutive chemical reactions; φ_1^2 = 0.4; φ_2^2 = 0.3; γ_1 = 20; γ_2 = 18; ε = 1; χ = 1.

Figure 8. Bifurcation diagrams for the yield of the intermediate product, y_B, of the consecutive chemical reactions; φ_1^2 = 0.4; φ_2^2 = 0.3; γ_1 = 20; γ_2 = 18; ε = 0.1; χ = 1.

Figure 9. Bifurcation diagrams for the yield of the intermediate product, y_B, of the consecutive chemical reactions; φ_1^2 = 0.4; φ_2^2 = 0.3; γ_1 = 20; γ_2 = 18; ε = 0.1; $\chi = 10^{-4}$.

Figure 10. Bifurcation diagrams for the effectiveness factor, η_B, for φ_1^2 = 0.4; φ_2^2 = 0.3; γ_1 = 20; γ_2 = 18; ε = 1; χ = 1.

Figure 11. Bifurcation diagrams for the effectiveness factor, η_B, for φ_1^2 = 0.4; φ_2^2 = 0.3; γ_1 = 20; γ_2 = 18; ε = 0.1; χ = 1.

Figure 12. Bifurcation diagrams for the effectiveness factor, η_B, for φ_1^2 = 0.4; φ_2^2 = 0.3; γ_1 = 20; γ_2 = 18; ε = 0.1; $\chi = 10^{-4}$.

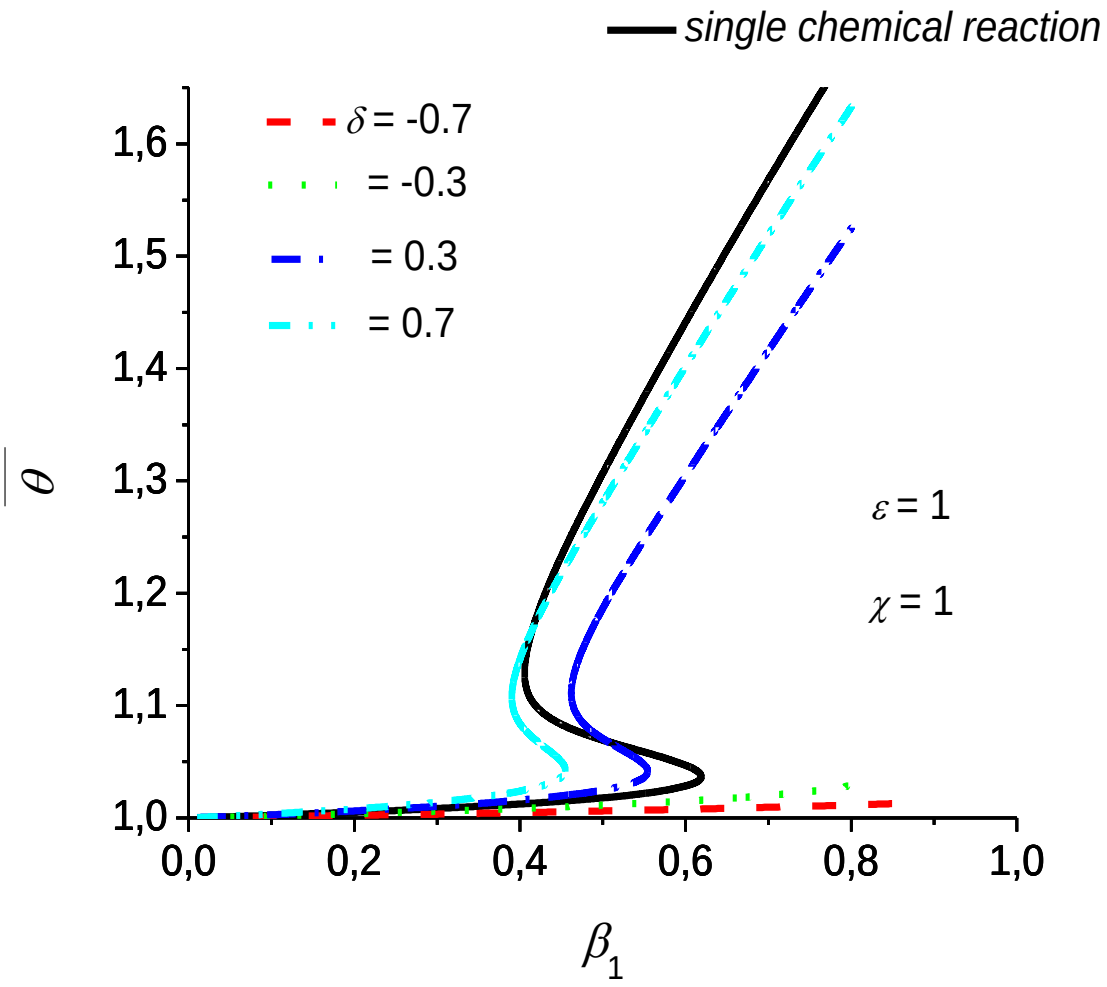

Figure 1.

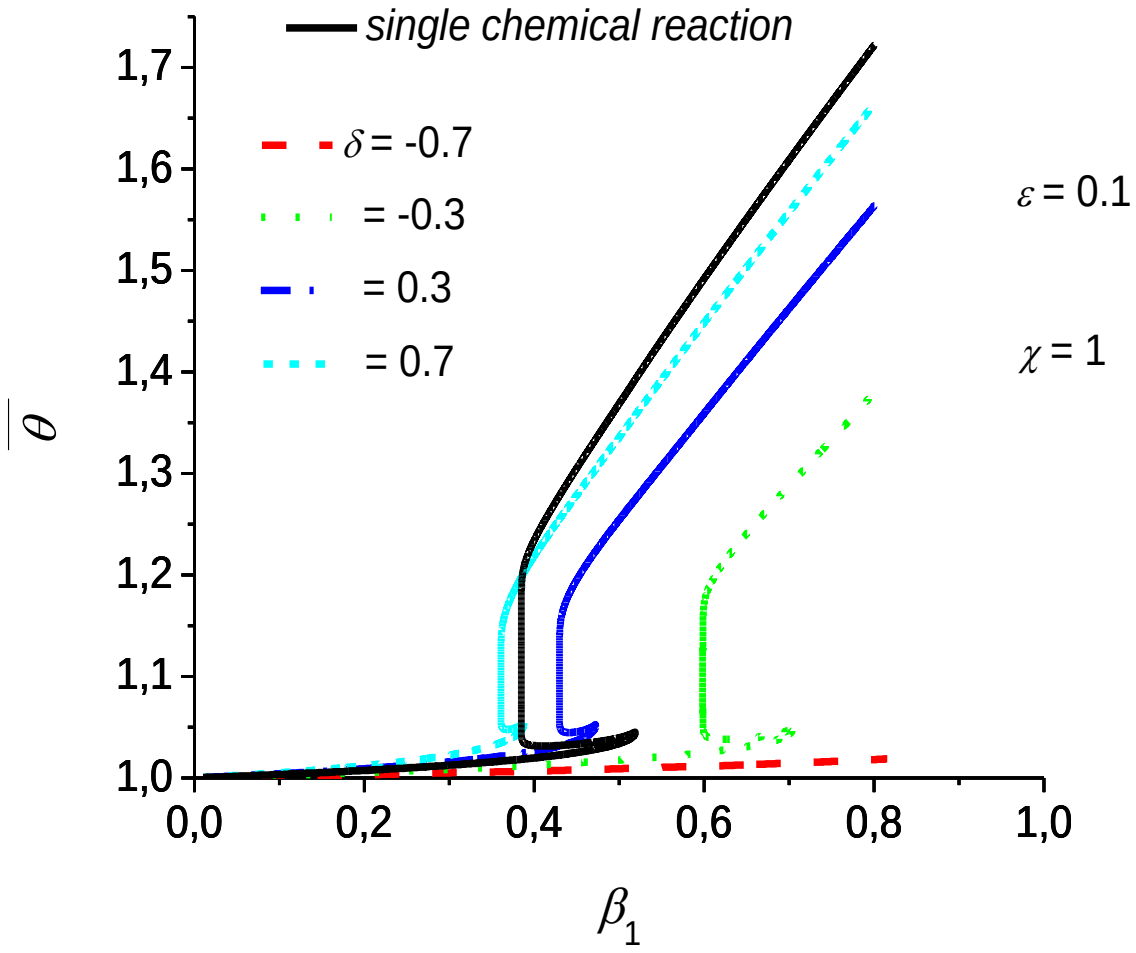

Figure 2.

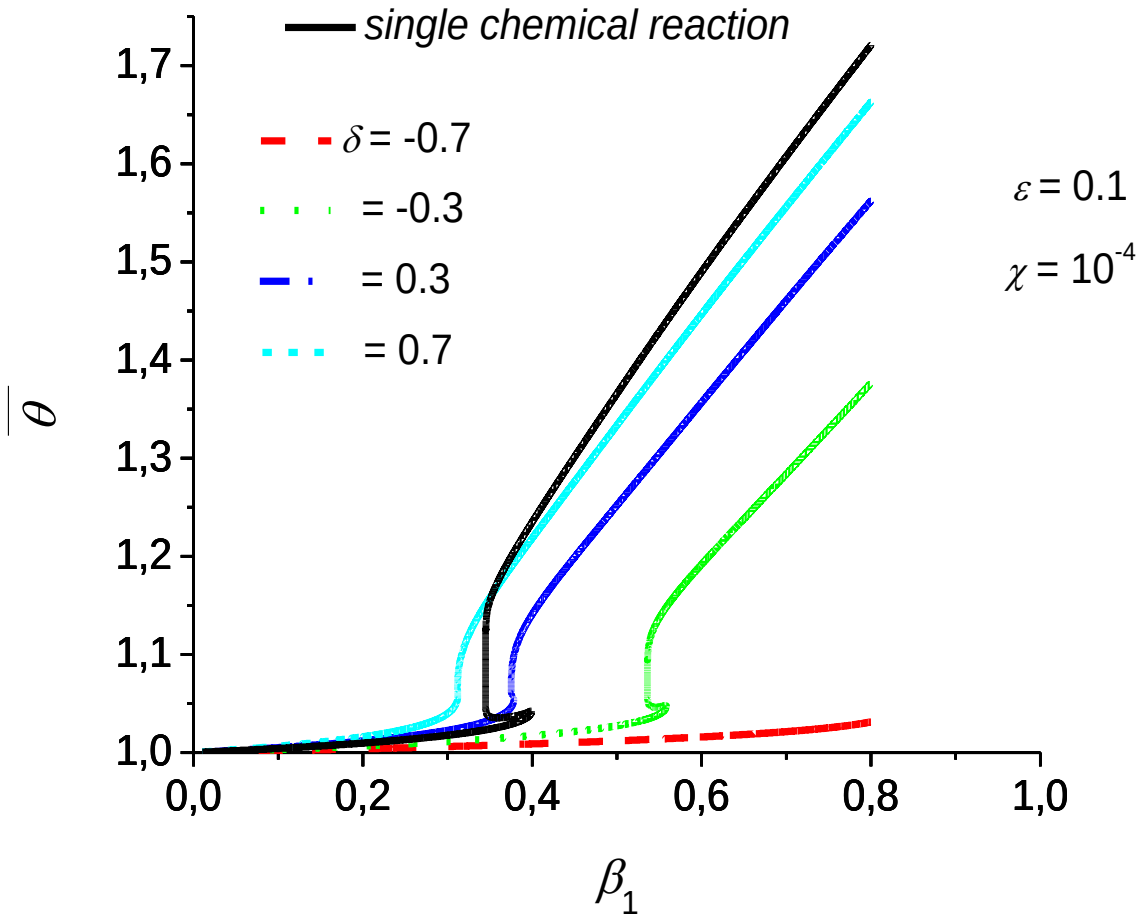

Figure 3.

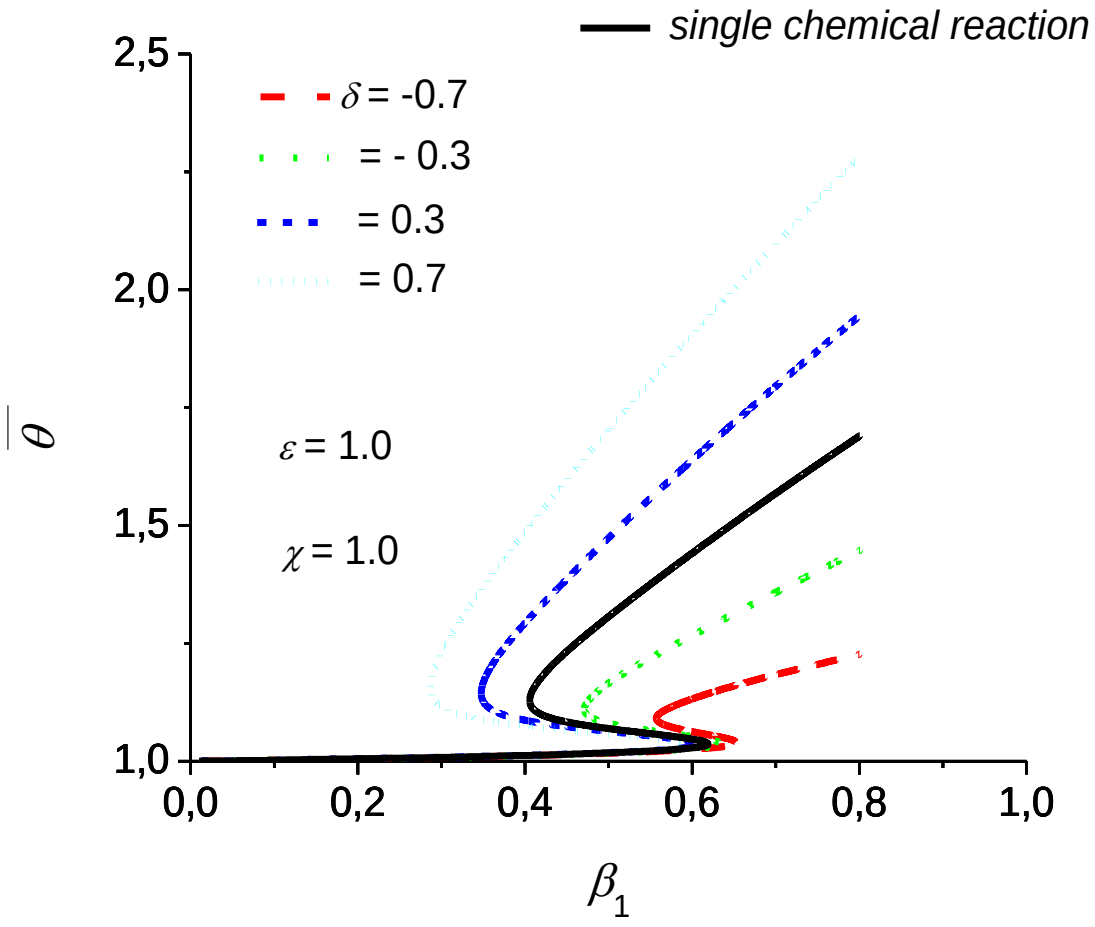

Figure 4.

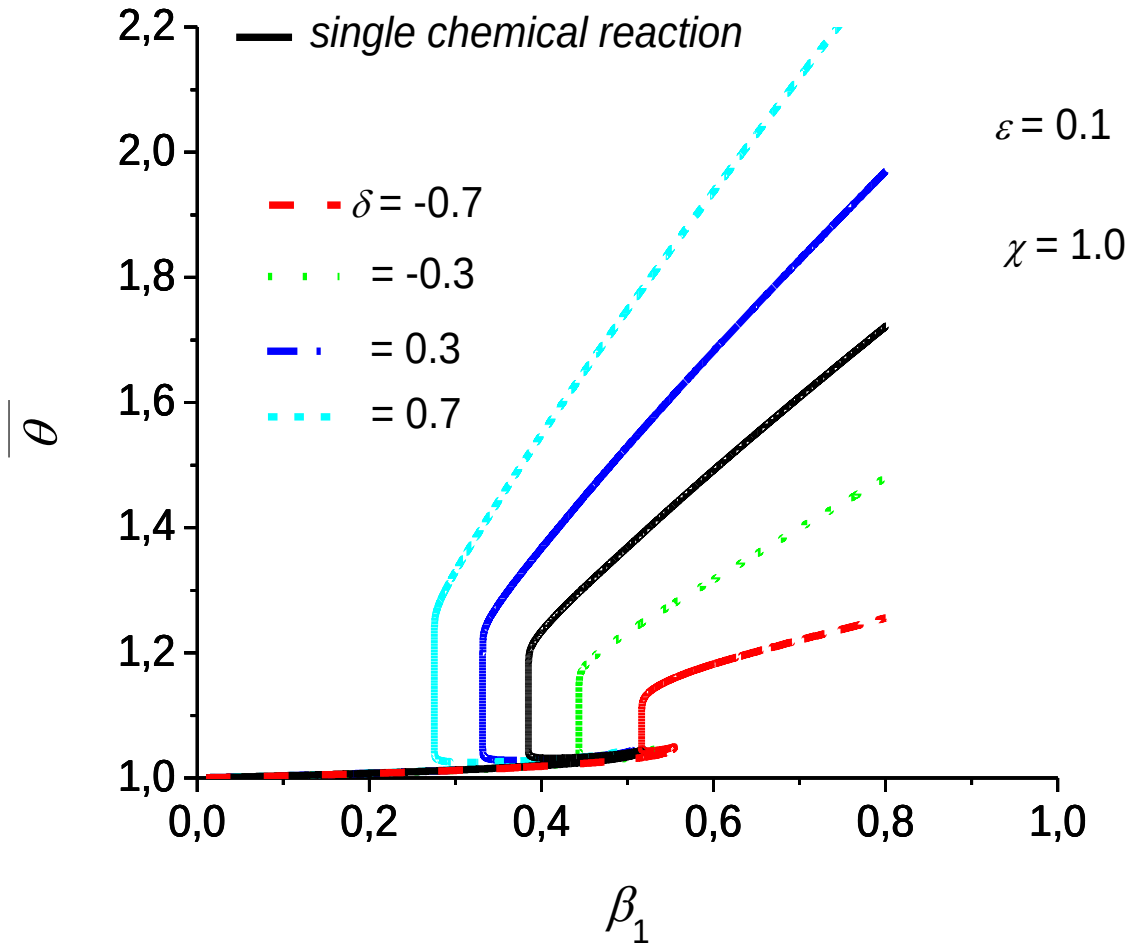

Figure 5.

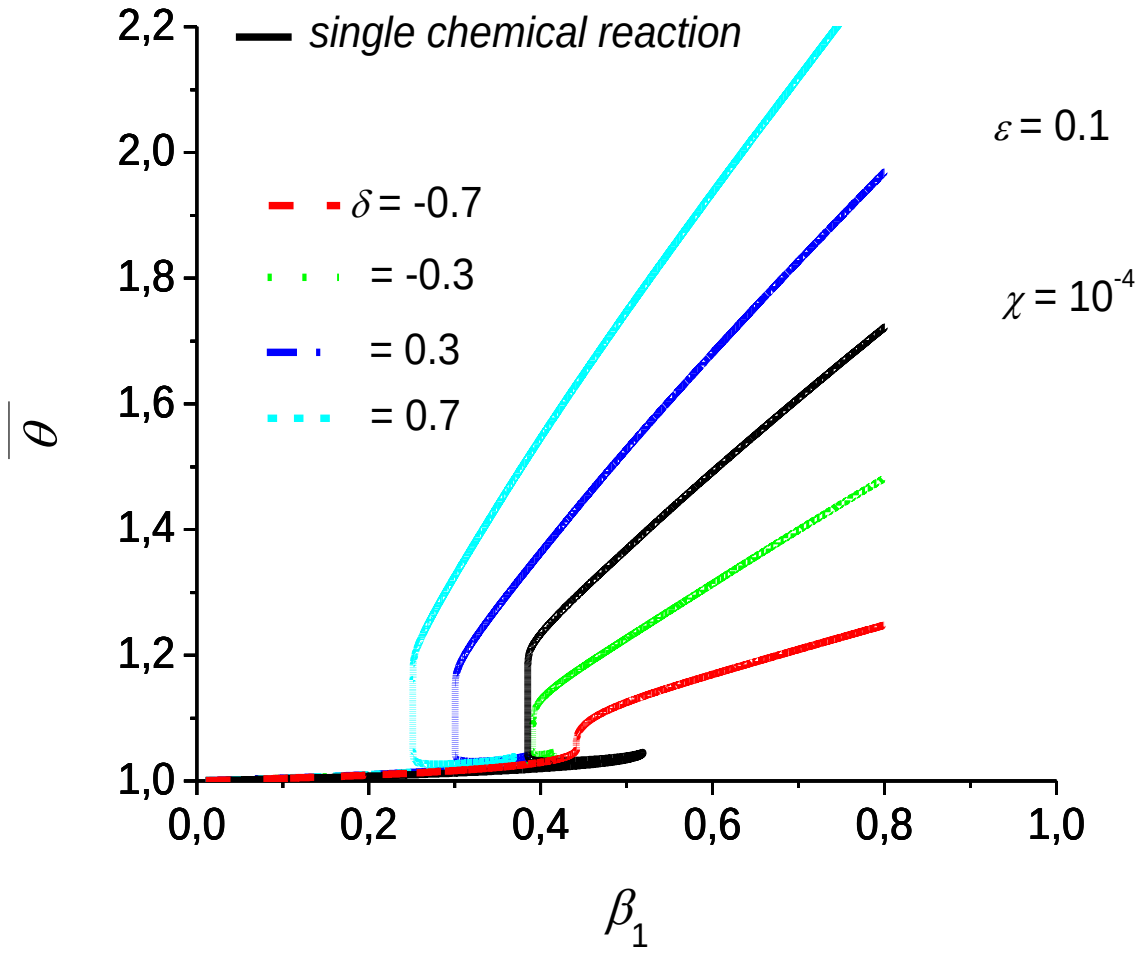

Figure 6.

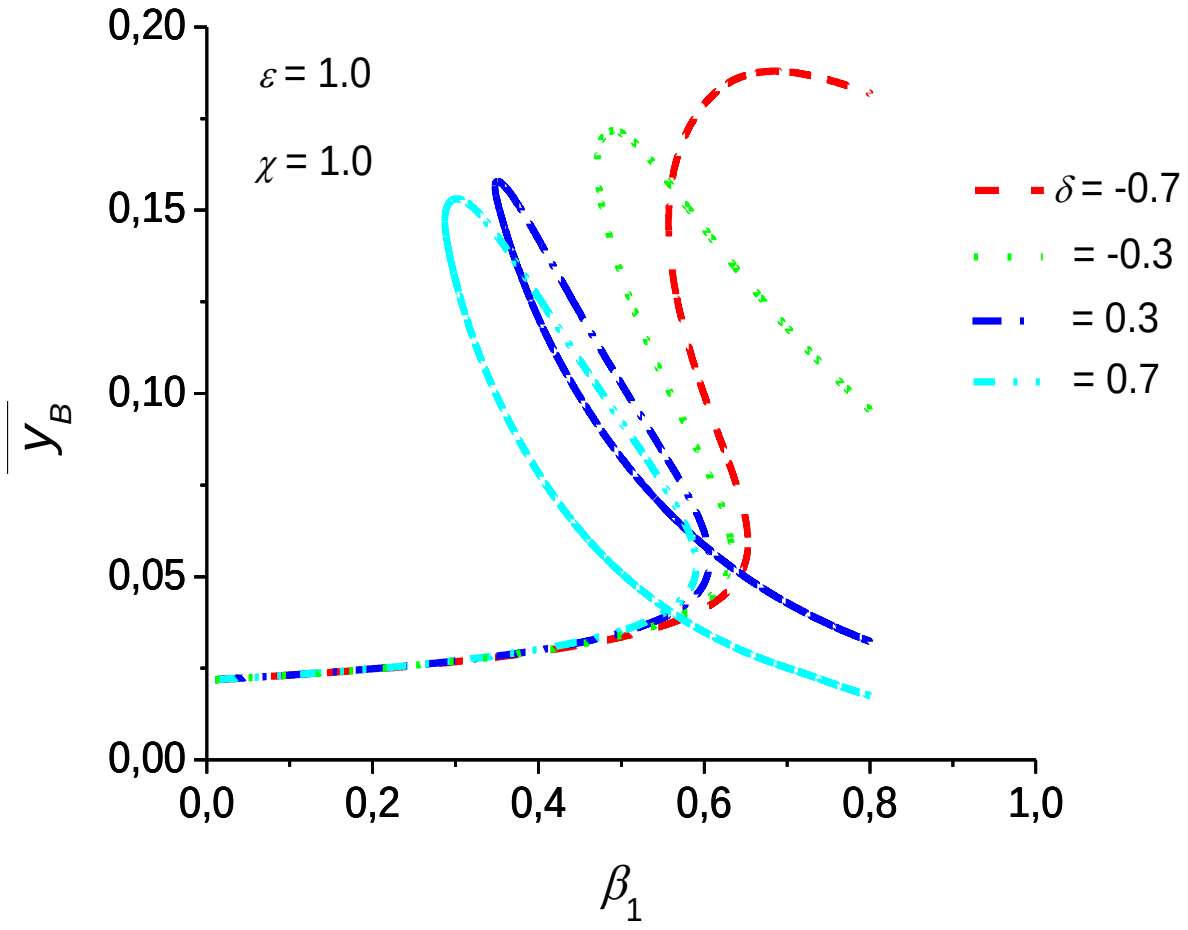

Figure 7.

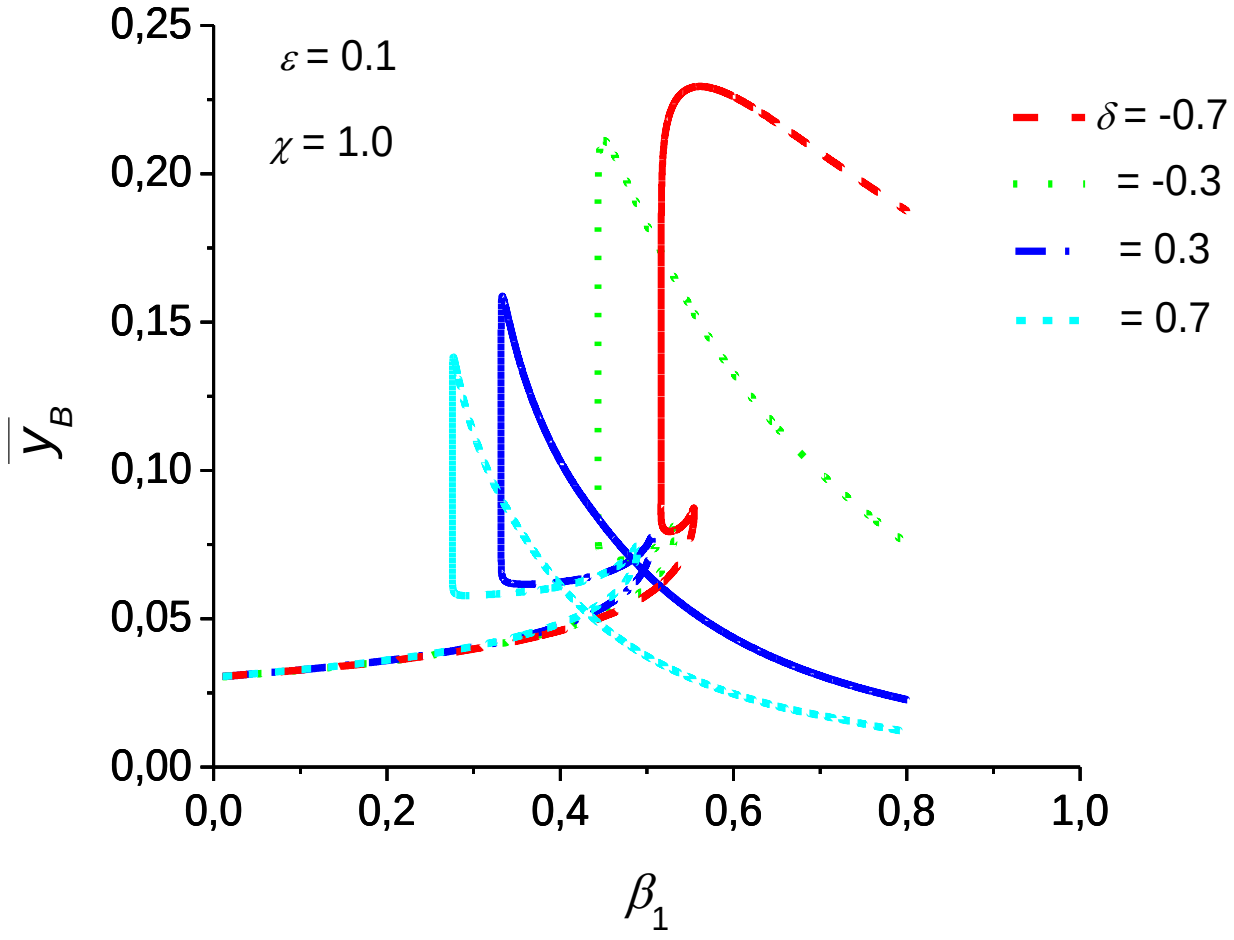

Figure 8.

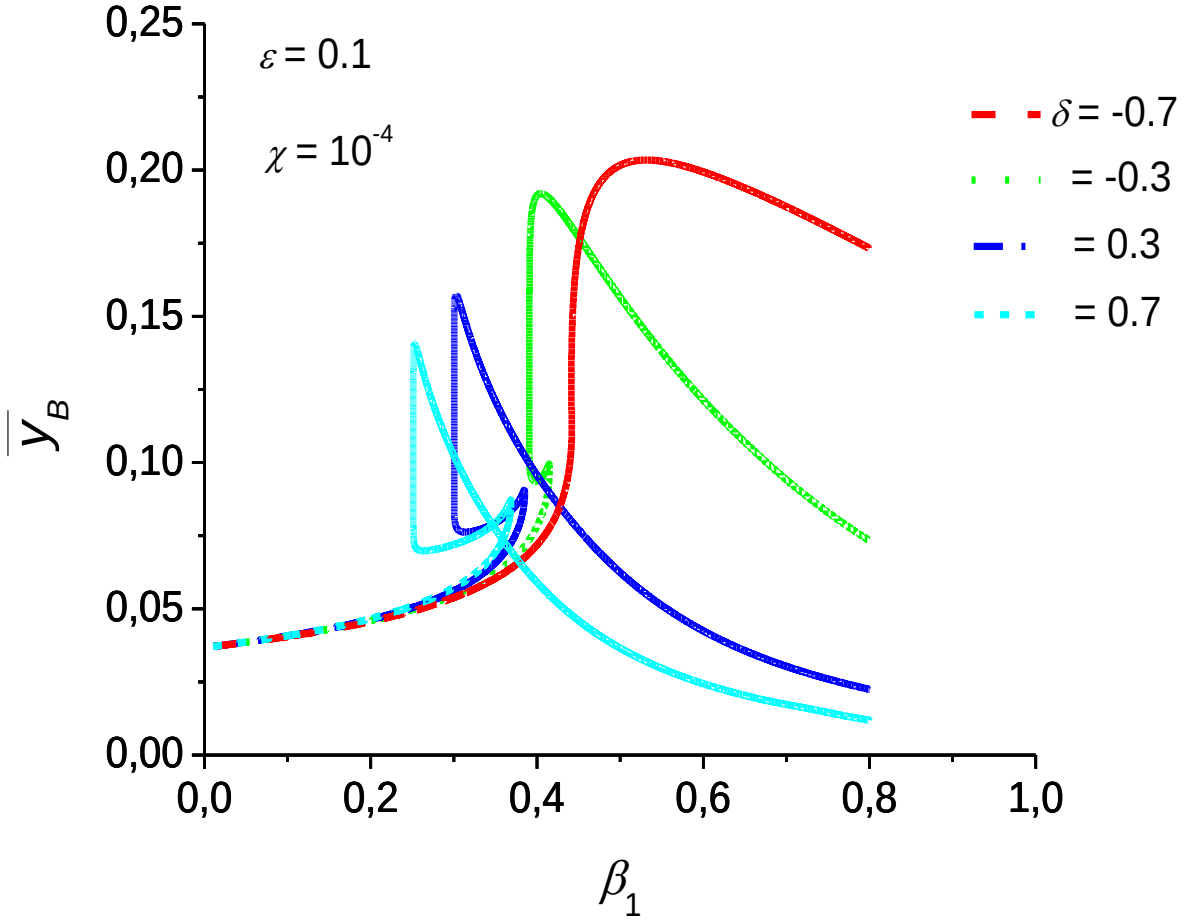

Figure 9.

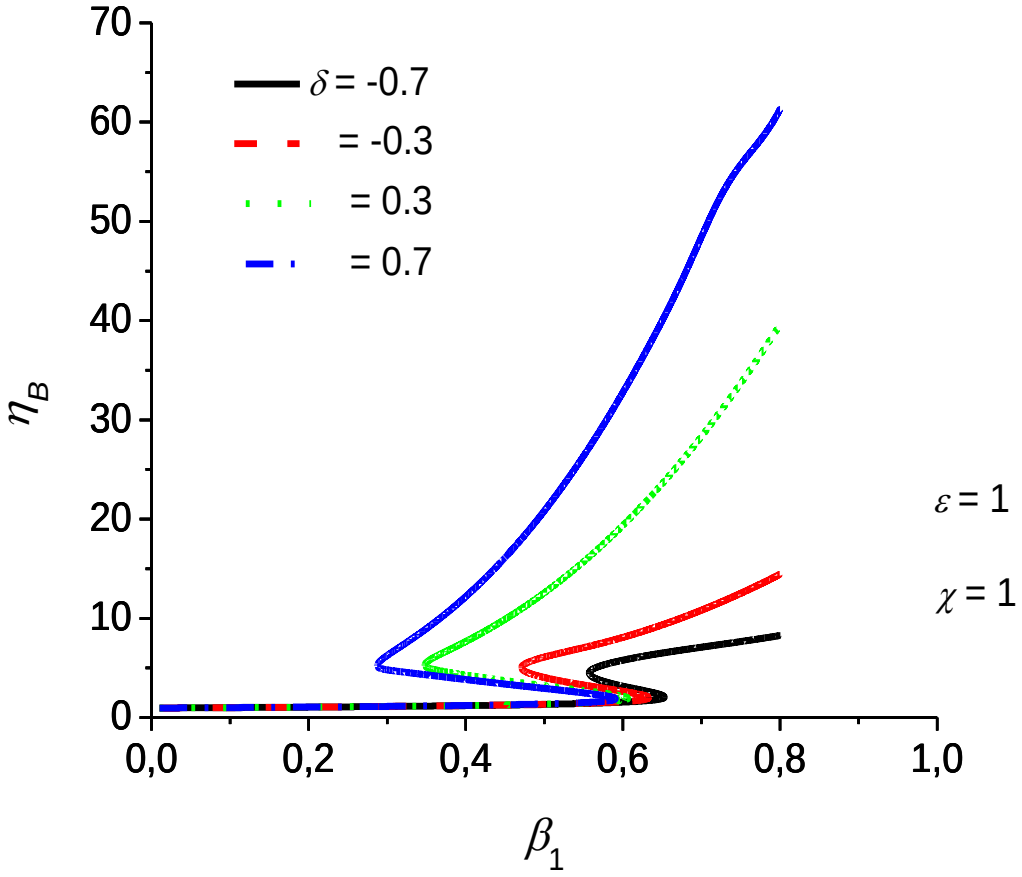

Figure 10.

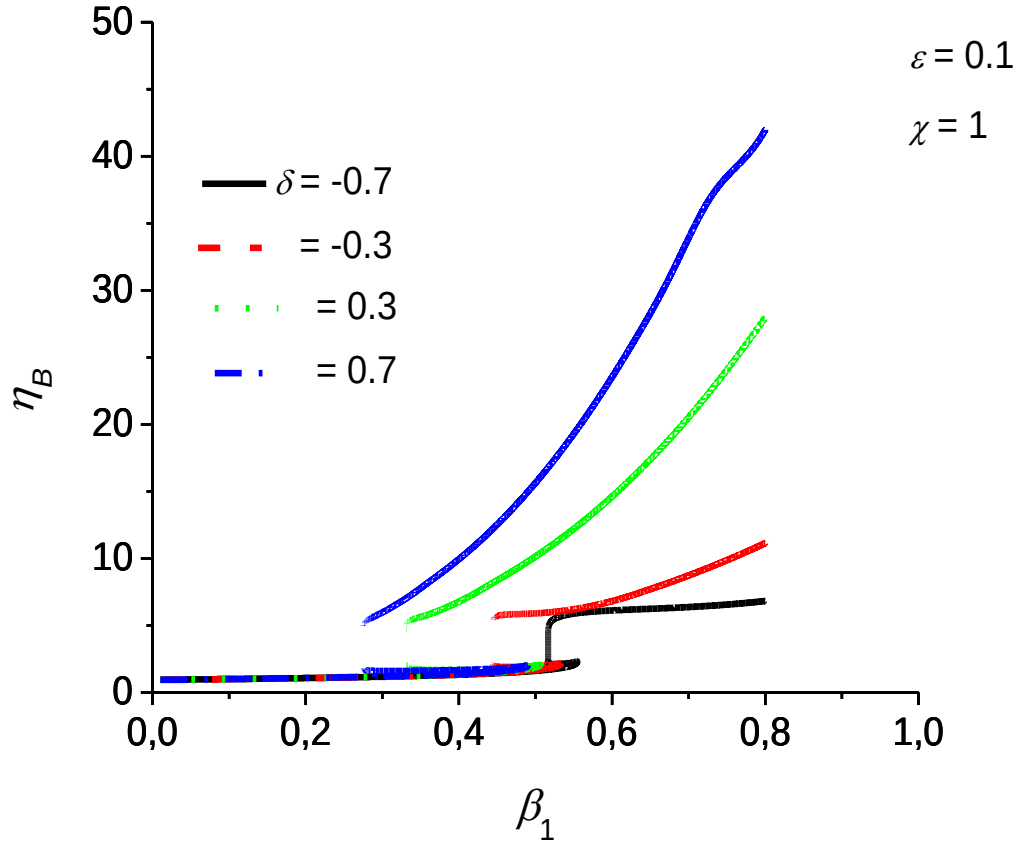

Figure 11.

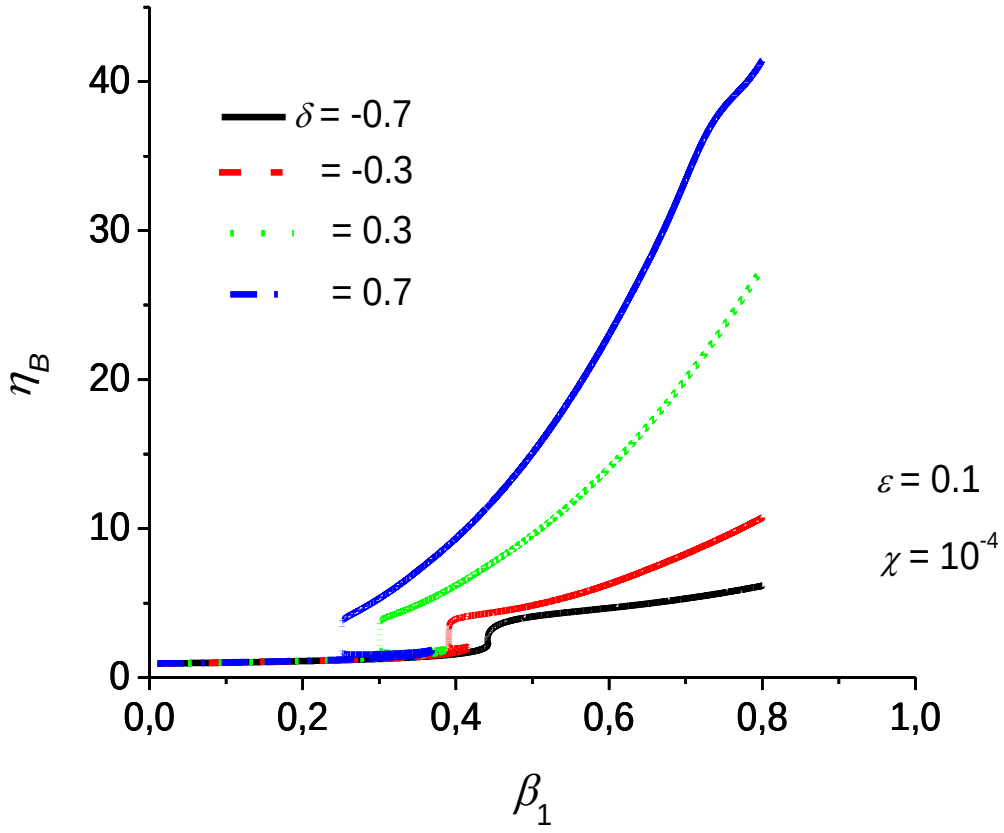

Figure 12.